**Wind and Structures**, *Vol. 19, No. 6 (2014) 623-647*
DOI: http://dx.doi.org/10.12989/was.2014.19.6.623 

# Prediction of negative peak wind pressures* on roofs of low-rise building

K. Balaji Rao*, M.B. Anoop, P. Harikrishna, S. Selvi Rajan and Nagesh R. Iyer

*CSIR-SERC, CSIR Campus, Taramani, Chennai 600 113, India*

*(Received April 15, 2014, Revised October 17, 2014, Accepted November 6, 2014)*

**Abstract.** In this paper, a probability distribution which is consistent with the observed phenomenon at the roof corner and, also on other portions of the roof, of a low-rise building is proposed. The model is consistent with the choice of probability density function suggested by the statistical thermodynamics of open systems and turbulence modelling in fluid mechanics. After presenting the justification based on physical phenomenon and based on statistical arguments, the fit of alpha-stable distribution for prediction of extreme negative wind pressure coefficients is explored. The predictions are compared with those actually observed during wind tunnel experiments (using wind tunnel experimental data obtained from the aerodynamic database of Tokyo Polytechnic University), and those predicted by using Gumbel minimum and Hermite polynomial model. The predictions are also compared with those estimated using a recently proposed non-parametric model in regions where stability criterion (in skewness-kurtosis space) is satisfied. From the comparisons, it is noted that the proposed model can be used to estimate the extreme peak negative wind pressure coefficients. The model has an advantage that it is consistent with the physical processes proposed in the literature for explaining large fluctuations at the roof corners.

**Keywords:** peak wind pressure coefficients; low-rise buildings;alpha-stable distribution

## 1. Introduction

It is known that when the small-scale turbulence associated with the incident wind interacts with low-rise buildings, it will result in large scale fluctuations of pressures induced on the roofs, especially nearer to regions of separation/vortex flow formation. Negative peak wind pressure coefficient of about -20 have been observed on the roof of the full scale experimental building at Texas Tech University (Tieleman 2003, Banks and Meroney 2001). Typically, the stochastic process associated with pressure fluctuations in the near portion of separation can exhibit wide-banded nature compared to the band width of incident wind turbulence spectrum (Kumar and Stathopoulos 2000). Depending on the mechanism of eddy formation (flow separation/vortex cone formation), location of pressure tap and angle of attack, for a given roof angle, generally negative pressure coefficients follow negatively skewed distributions. The large pressure fluctuations observed can be attributed to the flow separation (Bienkiewicz and Sun 1992) or initiation of large

∗Corresponding author, Scientist, E-mail: balajiserc1@yahoo.com
* The peak wind pressure here corresponds to the 1 second peaks of the recorded data and not the peaks of samples in an ensemble.


http://www.techno-press.org/?journal=was&subpage=8 ISSN: 1226-6116 (Print), 1598-6225 (Online)

vortices (Bienkiewicz and Sun 1992, Kawai and Nishimura 1996) depending on wind and roof angles.

Determination of an appropriate distribution for predicting the negative peaks of wind pressure coefficients on low-rise building roof is an active area of research (see for instance, Holmes and Cochran 2003, Cope *et al*. 2005, Yang *et al*. 2013). Cope *et al*. (2005) identified that different probability density function (pdf) models need to be used for wind pressures on different regions of the structure. Recent efforts are towards identification of a single model for the negative tails. Yang *et al*. (2013) proposed the use of Hermite polynomial model.

In the present investigation, applicability of alpha-stable distribution (Nolan 2009) for modeling the negative peak wind pressure coefficients on the roof corner regions and other portions of the roof of a low-rise gabled roof building is examined, using wind tunnel experimental data obtained from the aerodynamic database of Tokyo Polytechnic University (TPU 2013).

## 2. Negative peak wind pressure fluctuations on roofs of low-rise buildings

Different investigators have put forward hypotheses for explaining the large negative, intermittent peak pressures observed on the roofs of low-rise buildings (Tieleman 2003, Melbourne 1980, 1993, Banks and Meroney 2001). The reattachment of shear layer to the roof (which occurs for certain conditions of oncoming turbulence and angle of attack) causes the formation of separation bubble (see Fig. 1). The separation bubble is not steady and has two modes of pseudo-periodic unsteadiness (Blazawicz 2007), namely, the shedding mode and the flapping mode. The shedding mode is associated with the shedding of large-scale vortices downstream from the separation bubble with a frequency of about $0.65U/x_R$ (where, $U$ is the mean free stream flow velocity, and, $x_R$ is the mean length of separation bubble). The flapping mode is associated with the enlargement and contraction of the separation bubble and the flapping motion of the shear layer with a frequency of about $0.12U/x_R$, accompanied by the shedding of much larger vortices. The large negative pressures observed on the roofs are caused by the large pressure drops beneath the vortices as they convect downstream (see Fig. 2). The intermittent nature of shedding of vortices leads to jumps in the pressure time history at any given point on the roof. It has been also identified that both small- and large- scale oncoming turbulence influence the development of negative peak pressures (Tieleman 2003). This is because, in the presence of only small-scale turbulence, the vortices do not attain full maturity before they are convected downstream and hence maximum peak pressures are not felt. However, when large-scale turbulence is also present, the vortices attain maturity before being shed downstream leading to peak suction pressures of larger magnitudes.

The local environment near the corner of the roof can be modeled as a non-stationary and as a non-equilibrium thermodynamically open system. In such systems, it is known that the physical mechanisms generating the fluctuating forces are distinct from, and independent of, those generating dissipative forces. Hence, there may be no relation between fluctuations and dissipation, and such systems do not approach a thermodynamic equilibrium state asymptotically. More often, in such systems, the energy flux provided by the fluctuations may not be quenched by dissipation mechanism leading to instability (Lindenberg and West 1990). This will manifest in the form of jumps in the time histories of wind pressure coefficients. As pointed out by Fogarasi (2003), those non-gaussian distributions can be better modeled using Levy-alpha-stable distributions. The presence of multiple turbulence length scales contributing to the pressure fluctuation phenomenon at the roof corner is also evident from the spectrum of wind pressure presented in Fig. 7 of Kumar and Stathopoulos (2000). To account for these fluctuations in large negative peak pressures, attempts have been made to fit a suitable pdf for peak negative pressure coefficients, and propose an equation for design peak pressure that can be used in the design of components such as claddings (Holmes and Cochran 2003, Cope *et al*. 2005, Yang *et al*. 2013).

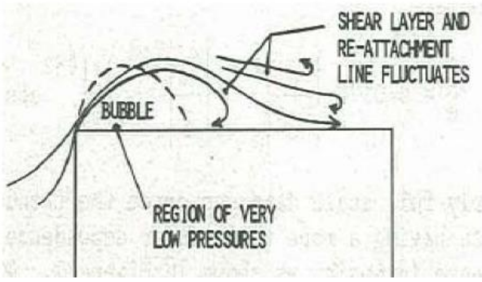


Fig. 1 Formation of separation bubble due to the reattachment of shear layer to the roof (from Melbourne 1980)

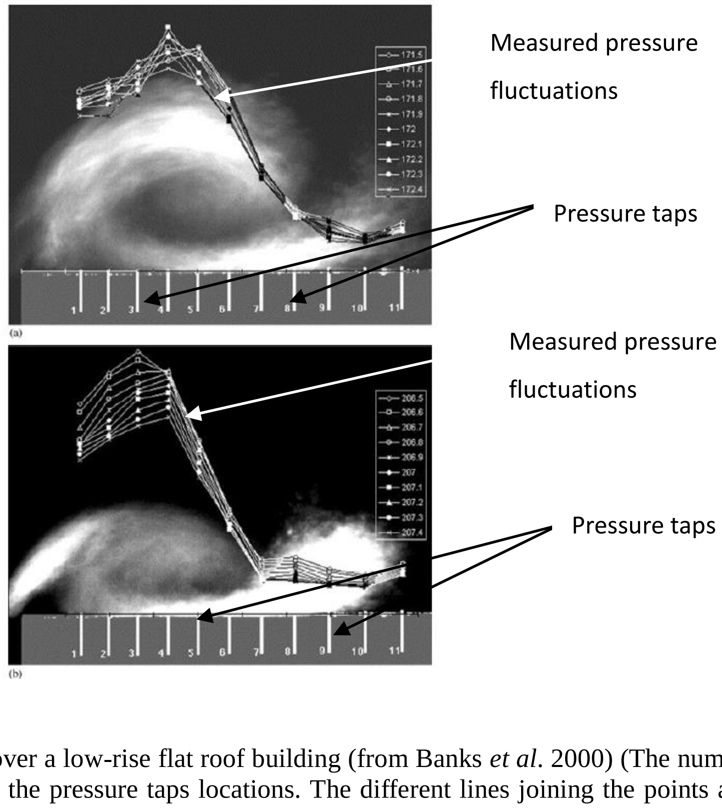


Fig. 2 Visualization of flow over a low-rise flat roof building (from Banks *et al*. 2000) (The numbers 1-11 at the bottom indicate the pressure taps locations. The different lines joining the points above the pressure taps represent the pressure fluctuations measured while the image of the vortex is being captured. The numbers in the legend indicate the time instants at which the surface pressures are recorded)

Narasimha *et al*. (2007), in a different context, studied the statistical characteristics of positive- and negative- fluxes in wall bounded flow turbulence in a nearly neutral atmospheric boundary layer, and found that the flow form coherent structures and exhibit burstiness, calling for a separate distribution other than that follows Fourier description. The intermittency/burstiness causes jumps and thus large local pressure fluctuations.

From the above discussion, it is clear that there is a need to use probability distributions with heavy tails to model these pressure fluctuations. It may be better to use distributions with power law decaying tails than exponential tails (which gives low values of probability to the tail regions) to predict very large pressures. One candidate distribution with power law decaying tails, which has found applications in different fields (Nolan 2009), is the alpha-stable distribution. In this paper, an attempt is made to study the applicability of alpha-stable distribution for modeling the negative peak wind pressure fluctuations on low-rise building roofs. The required wind pressure data is obtained from the aerodynamic database of Tokyo Polytechnic University.

## 3. Justification for use of alpha-stable distributions

The focus in this paper is to justify the use of alpha-stable distribution for modeling the negative peak wind pressure fluctuations on low-rise building roofs based on mechanics- and-phenomenological considerations and experimental observations. The motivation for the study is based on the following observations:

- The probability density functions of fluctuating pressures measured on a building model in a boundary layer wind tunnel are found to be negatively skewed with heavier negative tails and sharper peaks than normal distributions (Li *et al.* 1999). Hence, there is a need to use probability distributions with heavy tails to model the large pressure fluctuations and to estimate the extreme values. While there are number of heavy-tailed probability distributions, such as alpha-stable distribution, log-normal distribution, Student's t-distribution, hyperbolic distribution, the use of alpha-stable distribution is supported by the generalized central limit theorem. Log-normal distribution is another heavy tailed distribution which is found to be useful in large number of applications, and has also been used for modeling wind pressure fluctuations measured in wind tunnel experiments (Li *et al.* 1999). However, the applicability of log-normal distribution for pressure fluctuations consisting of both positive- and negative-pressures need to be carefully examined.
- Alpha-stable distributions are a rich class of probability distributions, which can accommodate fat tails and asymmetry (Nolan 2009). The normal-, Cauchy-, and Levy- distributions are special cases of alpha-stable distributions, suggesting the generality of alpha-stable distributions. Therefore, alpha-stable distribution will be a suitable candidate in the efforts towards identifying a single model for the peak wind pressure coefficients in different regions of the roof of a structure.
- For wind pressure measurement on a building model, the flow is assumed to be steady (i.e., long run behavior of fluctuations is same) and the process of pressure fluctuation is ergodic. In such a condition, the environment around the building envelope vary slowly but, the aerodynamic interaction provides a heterogeneous environment that would result in trapped and hopping behavior (observed in such systems) of pressure field. This is clear from typical time traces of pressure coefficients reported in literature. The trapped and hopping behavior of local pressure field results in complexity in the pressure process leading to anomalous

diffusion. The consistent distribution to model such a process is the long tailed Levy stable distribution (Metzler and Klafter 2004). As has been pointed out by Wang *et al.* (2012), the phenomenon underlying the observed stochastic pressure process can be modeled using Fickian non-Gaussian process. Their study considered a Gaussian central and non-Gaussian (exponential) tails for describing the probabilistic variations in displacements. It has also been pointed out that the application of non-Gaussian distributions such as alpha-stable distribution is going to be the future area of research. An exhaustive review of recent research needs in bluff body aerodynamics and the need to develop different modeling philosophies have been lucidly brought out by Kareem (2010).

## 4. Alpha-stable distribution - some preliminaries

For alpha-stable distribution, an explicit expression for pdf generally does not exist. The characteristic function of alpha-stable distribution is given by (Nolan 2009]

$$L_{\alpha,\beta}(t) = E[\exp(itX)] = \begin{cases} \exp\left\{-c^{\alpha}|t|^{\alpha}\left[1 - i\beta\, sign(t)\tan\left(\frac{\pi\alpha}{2}\right)\right] + i\delta t\right\}; \text{ for } \alpha \neq 1 \\ \exp\left\{-c|t|\left[1 + i\beta\, sign(t)\frac{2}{\pi}\ln|t|\right] + i\delta t\right\}; \text{ for } \alpha = 1 \end{cases} \tag{1}$$

where, $X$ - random variable, $i$ - imaginary unit, $t$ - argument of the characteristic function ($t \in \Re$), $E[.]$ - expected value, $\alpha$ - characteristic exponent or stability parameter ($\alpha \in (0,2]$), $\beta$ - skewness parameter ($\beta \in [-1,1]$), $c$ - scale parameter ($c > 0$), $\delta$ - location parameter ($\delta \in \Re$), ln - natural logarithm, and, *sign*($t$) - a logical function having values -1, 0, 1 for t < 0, t = 0 and t >0, respectively.

The lack of closed form expressions for probability density functions and/or probability distribution functions for general alpha-stable distributions have been pointed as the major drawback for the application of the same in practice. However, as noted by Nolan (2009), computer programs are now available for computation of probability densities, probability distributions and quantiles. Also, number of methods have been proposed by different researchers for the estimations of the parameters (namely, $\alpha$, $\beta$, $c$ and $\delta$) of the alpha-stable distribution (see Balaji Rao *et al*. (2013) for a brief survey). These facilitate the practical applications of alpha-stable distributions.

## 5. Wind pressure coefficient data (from TPU 2013)

In this study, an attempt is made to examine the applicability of alpha-stable distribution to model the peak wind pressure coefficients on the roof corner regions and other portions of the roof of a low-rise gabled roof building, using wind tunnel experimental data from the aerodynamic database of Tokyo Polytechnic University (TPU 2013). Salient information regarding the experimental investigations is as follows. The test model considered is gabled roof with eave height (H0) of 80 mm, breadth (B) of 160 mm and depth (D) of 400 mm (see Fig. 3). In the present study, the roof pitch angles considered are 0°, 4.8°, 9.4° and 14°, and, the wind angle of attack (θ) considered are 0°, 45° and 90°. The tested wind field was the suburban terrain corresponding to terrain category III of AIJ (TPU 2013). The turbulence intensity and the test wind velocity at a height of 100 mm were about 0.25 and 7.4 m/s, respectively. The wind pressure taps were placed as shown in Fig. 3. Total number of pressure taps was 210 for all roof pitch angles except for $14^{o}$. The sampling frequency was 500 Hz and the sampling period was 18 seconds for each sample (which corresponds to 15 Hz and 600 seconds, respectively, in full scale, based on simulated length scale of 1:100 and assumed velocity scale of 1:3). The time history of wind pressure coefficients (ratio of the measured wind pressure to the reference wind pressure of the approaching wind velocity at the average roof height, H) for each of the taps were moving averaged at every 0.006s (corresponding to 0.2s in full scale), and, are given in a database. The effective frontal area associated with 0.2-second moving average gust for the range of mean wind speeds of interest to the structural designers considered is about 10 $m^2$ to 40 $m^2$ (Ginger and Fricke 2012), which is in the order of the area of one cladding sheet on the roof of the building. Hence, the 0.2-second moving average gusts are considered in the present study.

## 6. Statistical analysis of peak wind pressure coefficients

The time histories of wind pressure coefficients ($C_p$) corresponding to the taps 72, 32, 82, 51, 52, 54 and 56 for θ = 0° and 90°, and, taps 72, 52, 54, 56, 32, 73 and 74 for θ = 45°, are considered in the study. It can be noted from Fig. 3 that most of these pressure taps correspond to roof corner where either flow separation would take place or along which conical vertices may initiate. The 1-second peak negative wind pressure coefficients ($\check{C}_p$) are obtained (the duration of 1 second is adopted adhocly), and the alpha-stable distribution and Gumbel minimum distribution (which is proposed by Tieleman *et al*. (2008) for peak suction pressures in separation regions of low-rise structures) are fitted to $\check{C}_p$. Here, 1-second peak corresponds to the 1 second peak in the full-scale. In the present study, the parameters of alpha-stable distribution are determined using the procedure proposed by Koutrouvelis (1980). (A brief discussion on the estimation of parameters of alpha-stable distribution is presented in Appendix).

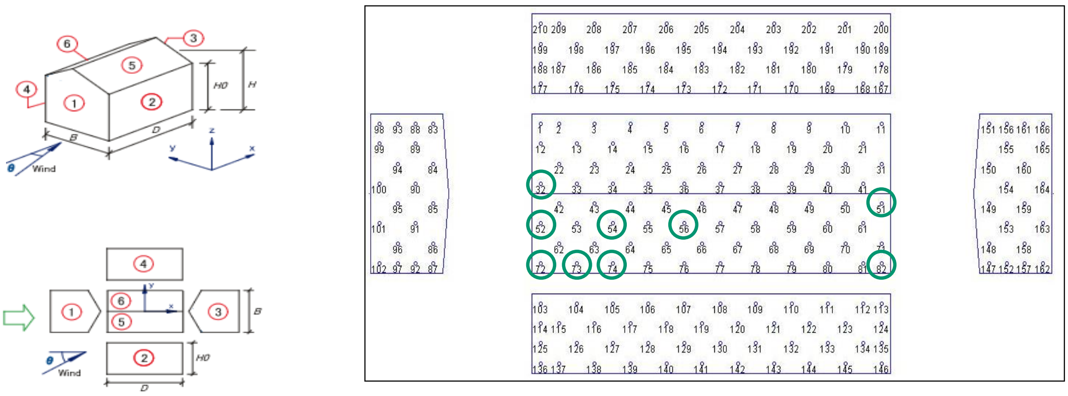

Location of taps (circles indicate the taps considered in the present study)

Fig. 3 Test model considered and locations of wind pressure taps (TPU 2013)

Recently, Yang *et al*. (2013) have proposed a Hermite polynomial-based model for modeling the non-Gaussian pressure variation on roofs of low-rise buildings. This method is a promising approach for data driven probabilistic modeling as pointed out by Fogarasi (2003). It is a non-parametric approach, requiring establishing regions of stability for moments of random variable. Peng *et al.* (2014) presented a method to obtain the refined points for which Hermite polynomial can be fitted for the points slightly away from the stability region. An attempt has been made in this paper to compare the predictions made by using alpha-stable distribution with that of Hermite polynomial model (Yang *et al*. 2013, Peng *et al.* 2014), for regions wherein stability conditions are satisfied.

## 7. Results and discussion

The time history and frequencies of experimentally determined wind pressure coefficients, typically for measurement tap 72, for roof pitch angle of 0° and θ = 90°, are shown in Figs. 4(a) and 4(b), respectively. The large negative pressure coefficients seen in Fig. 4(a) indicate the formation of large pressure drops due to the intermittent nature of shedding of vortices leading to jumps in the pressure time history. In Fig. 4(b) and also in following portion of the paper, '*observed*' denotes the wind pressure coefficients computed from the measured wind pressures in the wind tunnel experiments. The frequencies determined assuming wind pressure coefficients follow normal distribution is also shown in Fig. 4(b), for the purpose of comparison. From Fig. 4(b), it is noted that, as expected, the distribution of wind pressure coefficients is negatively skewed and the assumption of normal distribution for wind pressure coefficients is not appropriate.

The statistical properties (namely, mean, standard deviation, skewness and kurtosis) of 1-second peak negative wind pressure coefficients ($\check{C}_p$) have been computed, and are given in Table 1. The values of parameters of the alpha-stable- and Gumbel minimum- distributions, fitted to $\check{C}_p$, are also given in Table 1. (A brief discussion on the estimation of parameters of alpha-stable distribution is presented in Appendix).

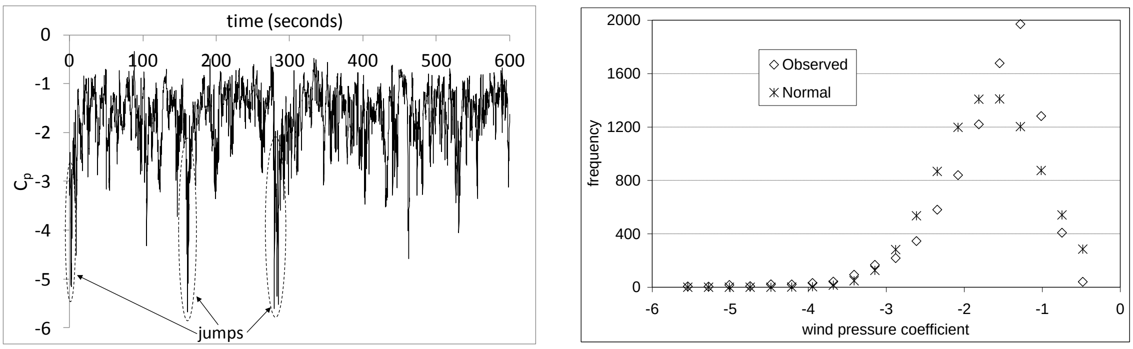


(a) (b)

Fig. 4 (a) Time history- and (b) Frequency distribution- of wind pressure coefficients for measurement tap 72 (roof pitch angle = 0°, θ = 90°)

Table 1 Statistical properties of 1-second peak wind pressure coefficients and parameters of fitted alpha-stable and Gumbel minimum distributions

| Measurement tap | θ (°) | Roof pitch angle (°) | wind pressure coefficients | | | | | | | | | | Applicability of Hermite polynomial model[5] |
|---|---|---|---|---|---|---|---|---|---|---|---|---|---|
| | | | statistical properties | | | | parameters of alpha-stable distribution | | | | parameters of Gumbel minimum distribution[4] | | |
| | | | mean | SD[1] | Skew[2] | Kurt[3] | $\alpha$ | $\beta$ | $c$ | $\delta$ | $\gamma$ | $\mu$ | |
| 32 | 0 | 0 | -1.31 | 0.49 | -1.08 | 1.59 | 1.84 | -1 | 0.30 | -1.35 | 0.38 | -1.09 | No |
| | | 4.8 | -1.31 | 0.57 | -1.64 | 4.76 | 1.67 | -1 | 0.31 | -1.38 | 0.44 | -1.06 | Yes |
| | | 9.4 | -1.44 | 0.59 | -1.06 | 0.97 | 1.76 | -1 | 0.36 | -1.50 | 0.46 | -1.18 | No |
| | | 14 | -1.24 | 0.52 | -1.09 | 1.27 | 1.74 | -1 | 0.31 | -1.30 | 0.41 | -1.01 | No |
| | 90 | 0 | -0.88 | 0.35 | -1.18 | 1.81 | 1.66 | -1 | 0.20 | -0.92 | 0.28 | -0.72 | No |
| | | 4.8 | -0.81 | 0.27 | -1.15 | 3.08 | 1.87 | -1 | 0.17 | -0.82 | 0.21 | -0.68 | Yes |
| | | 9.4 | -0.96 | 0.30 | -0.99 | 1.98 | 1.82 | -1 | 0.19 | -0.98 | 0.24 | -0.83 | Yes |
| | | 14 | -1.17 | 0.38 | -1.01 | 1.56 | 1.78 | -1 | 0.24 | -1.19 | 0.30 | -0.99 | No |
| 51 | 0 | 0 | -0.26 | 0.11 | -0.36 | -0.13 | 2.00 | -* | 0.08 | -0.26 | 0.09 | -0.21 | No |
| | | 4.8 | -0.25 | 0.11 | -0.43 | 0.62 | 1.91 | -1 | 0.07 | -0.25 | 0.09 | -0.20 | Yes |
| | | 9.4 | -0.26 | 0.11 | -0.31 | 0.32 | 1.96 | -1 | 0.08 | -0.26 | 0.09 | -0.21 | Yes |
| | | 14 | -0.25 | 0.10 | -0.28 | 0.32 | 1.96 | -1 | 0.07 | -0.25 | 0.08 | -0.20 | Yes |
| | 90 | 0 | -1.02 | 0.38 | -1.02 | 1.79 | 1.83 | -1 | 0.23 | -1.05 | 0.30 | -0.85 | Yes |
| | | 4.8 | -0.86 | 0.29 | -0.80 | 0.72 | 1.89 | -1 | 0.19 | -0.88 | 0.22 | -0.73 | No |
| | | 9.4 | -0.91 | 0.30 | -1.56 | 6.15 | 1.81 | -1 | 0.18 | -0.93 | 0.24 | -0.77 | Yes |
| | | 14 | -0.88 | 0.26 | -0.88 | 0.92 | 1.88 | -1 | 0.17 | -0.90 | 0.20 | -0.77 | No |
| 72 | 0 | 0 | -1.57 | 0.65 | -1.29 | 2.27 | 1.75 | -1 | 0.39 | -1.63 | 0.51 | -1.28 | No |
| | | 4.8 | -1.59 | 0.72 | -1.12 | 1.64 | 1.78 | -1 | 0.44 | -1.66 | 0.56 | -1.27 | No |
| | | 9.4 | -1.68 | 0.74 | -1.58 | 3.78 | 1.63 | -1 | 0.39 | -1.76 | 0.58 | -1.35 | No |
| | | 14 | -1.49 | 0.70 | -1.47 | 3.73 | 1.69 | -1 | 0.39 | -1.57 | 0.54 | -1.18 | Yes |
| | 90 | 0 | -2.04 | 0.78 | -1.51 | 3.47 | 1.67 | -1 | 0.43 | -2.12 | 0.61 | -1.69 | No |
| | | 4.8 | -2.21 | 0.74 | -0.67 | 0.37 | 1.95 | -1 | 0.51 | -2.23 | 0.58 | -1.88 | No |
| | | 9.4 | -2.33 | 0.73 | -0.88 | 1.48 | 1.86 | -1 | 0.46 | -2.38 | 0.57 | -2.00 | Yes |
| | | 14 | -1.86 | 0.62 | -1.03 | 1.52 | 1.66 | -1 | 0.35 | -1.94 | 0.48 | -1.59 | No |
| 82 | 0 | 0 | -0.27 | 0.15 | -1.14 | 3.07 | 1.86 | -1 | 0.09 | -0.28 | 0.12 | -0.20 | Yes |

| | | | | | | | | | | | | | |
|---|---|---|---|---|---|---|---|---|---|---|---|---|---|
| | | 4.8 | -0.26 | 0.14 | -0.96 | 2.44 | 1.83 | -1 | 0.08 | -0.27 | 0.11 | -0.20 | Yes |
| | | 9.4 | -0.27 | 0.14 | -1.20 | 4.28 | 1.85 | -1 | 0.09 | -0.27 | 0.11 | -0.21 | Yes |
| | | 14 | -0.25 | 0.12 | -0.65 | 1.46 | 1.93 | -1 | 0.08 | -0.25 | 0.09 | -0.19 | Yes |
| | 90 | 0 | -1.84 | 0.77 | -1.26 | 2.20 | 1.72 | -1 | 0.45 | -1.92 | 0.60 | -1.49 | No |
| | | 4.8 | -2.37 | 0.89 | -0.59 | 0.10 | 2.00 | -* | 0.63 | -2.37 | 0.69 | -1.97 | No |
| | | 9.4 | -2.24 | 0.82 | -1.45 | 4.81 | 1.81 | -1 | 0.49 | -2.27 | 0.64 | -1.87 | Yes |
| | | 14 | -1.91 | 0.61 | -0.56 | 0.31 | 1.96 | -1 | 0.42 | -1.92 | 0.48 | -1.63 | No |
| 32 | 45 | 0 | -1.64 | 0.48 | -0.46 | -0.20 | 1.99 | -1 | 0.34 | -1.65 | 0.37 | -1.42 | No |
| 52 | 45 | 0 | -2.21 | 0.80 | -0.52 | 0.09 | 1.99 | -1 | 0.56 | -2.22 | 0.62 | -1.85 | No |
| 72 | 45 | 0 | -0.94 | 0.49 | -2.80 | 12.29 | 1.47 | -1 | 0.19 | -1.00 | 0.38 | -0.72 | Yes |
| 73 | 45 | 0 | -2.41 | 0.75 | -0.75 | 1.26 | 1.90 | -1 | 0.49 | -2.45 | 0.59 | -2.08 | Yes |
| 74 | 45 | 0 | -1.82 | 0.51 | -0.76 | 0.79 | 1.92 | -1 | 0.34 | -1.85 | 0.40 | -1.59 | No |
| 52 | 0 | 0 | -1.35 | 0.51 | -1.38 | 3.41 | 1.77 | -1 | 0.30 | -1.39 | 0.40 | -1.12 | Yes |
| 54 | 0 | 0 | -0.54 | 0.23 | -0.80 | 1.40 | 1.90 | -1 | 0.15 | -0.55 | 0.18 | -0.44 | Yes |
| 56 | 0 | 0 | -0.27 | 0.14 | -0.47 | 0.30 | 1.99 | -1 | 0.10 | -0.27 | 0.12 | -0.20 | No |
| 52 | 90 | 0 | -1.45 | 0.44 | -1.09 | 1.61 | 1.78 | -1 | 0.27 | -1.48 | 0.34 | -1.25 | No |
| 54 | 90 | 0 | -1.58 | 0.49 | -1.05 | 1.39 | 1.80 | -1 | 0.30 | -1.63 | 0.38 | -1.35 | No |
| 56 | 90 | 0 | -1.57 | 0.52 | -1.30 | 2.38 | 1.67 | -1 | 0.29 | -1.63 | 0.41 | -1.34 | No |
| 52 | 45 | 0 | -2.21 | 0.80 | -0.52 | 0.09 | 1.99 | -1 | 0.56 | -2.22 | 0.62 | -1.85 | No |
| 54 | 45 | 0 | -0.55 | 0.39 | -2.00 | 4.70 | 1.25 | -1 | 0.14 | -0.77 | 0.30 | -0.38 | No |
| 56 | 45 | 0 | -1.16 | 0.50 | -0.38 | -0.24 | 2.00 | -1 | 0.36 | -1.17 | 0.39 | -0.93 | No |
| 52 | 0 | 4.8 | -1.37 | 0.59 | -1.35 | 2.69 | 1.68 | -1 | 0.33 | -1.44 | 0.45 | -1.11 | No |
| 54 | 0 | 4.8 | -0.57 | 0.28 | -1.62 | 5.26 | 1.71 | -1 | 0.15 | -0.60 | 0.22 | -0.45 | Yes |
| 56 | 0 | 4.8 | -0.27 | 0.15 | -0.54 | 0.60 | 1.94 | -1 | 0.10 | -0.27 | 0.11 | -0.20 | Yes |
| 52 | 90 | 4.8 | -1.05 | 0.35 | -0.79 | 0.63 | 1.91 | -1 | 0.23 | -1.07 | 0.27 | -0.89 | No |
| 54 | 90 | 4.8 | -1.42 | 0.47 | -0.89 | 1.55 | 1.90 | -1 | 0.30 | -1.44 | 0.36 | -1.21 | Yes |
| 56 | 90 | 4.8 | -1.55 | 0.50 | -0.42 | 0.04 | 2.00 | -1 | 0.35 | -1.56 | 0.39 | -1.32 | No |
| 52 | 45 | 4.8 | -2.17 | 0.90 | -0.93 | 1.36 | 1.86 | -1 | 0.57 | -2.23 | 0.71 | -1.76 | Yes |
| 54 | 45 | 4.8 | -0.56 | 0.35 | -1.75 | 3.29 | 1.27 | -1 | 0.13 | -0.71 | 0.27 | 0.40 | No |
| 56 | 45 | 4.8 | -1.01 | 0.47 | -0.70 | 0.27 | 1.96 | -1 | 0.33 | -1.03 | 0.37 | -0.80 | No |
| 52 | 0 | 9.4 | -1.49 | 0.59 | -1 | 0.99 | 1.79 | -1 | 0.37 | -1.54 | 0.46 | -1.23 | No |

| | | | | | | | | | | | | | |
|---|---|---|---|---|---|---|---|---|---|---|---|---|---|
| 54 | 0 | 9.4 | -0.66 | 0.31 | -0.97 | 1.42 | 1.86 | -1 | 0.19 | -0.68 | 0.24 | -0.52 | No |
| 56 | 0 | 9.4 | -0.29 | 0.16 | -0.77 | 1.65 | 1.86 | -1 | 0.10 | -0.30 | 0.13 | -0.22 | Yes |
| 52 | 90 | 9.4 | -0.88 | 0.31 | -1.24 | 2.38 | 1.75 | -1 | 0.18 | -0.91 | 0.24 | -0.74 | No |
| 54 | 90 | 9.4 | -1.24 | 0.44 | -1.55 | 4.95 | 1.74 | -1 | 0.26 | -1.27 | 0.35 | -1.04 | Yes |
| 56 | 90 | 9.4 | -1.34 | 0.47 | -1.15 | 1.69 | 1.74 | -1 | 0.28 | -1.39 | 0.37 | -1.13 | No |
| 52 | 45 | 9.4 | -1.87 | 0.87 | -0.54 | 0.24 | 1.99 | -1 | 0.61 | -1.88 | 0.68 | -1.48 | No |
| 54 | 45 | 9.4 | -0.54 | 0.27 | -2.07 | 6.42 | 1.50 | -0.97 | 0.12 | -0.57 | 0.21 | -0.41 | No |
| 56 | 45 | 9.4 | -0.91 | 0.43 | -1.31 | 1.91 | 1.55 | -1 | 0.22 | -0.99 | 0.33 | -0.72 | No |
| 52 | 0 | 14 | -1.29 | 0.55 | -1.09 | 1.34 | 1.78 | -1 | 0.34 | -1.34 | 0.43 | -1.04 | No |
| 54 | 0 | 14 | -0.53 | 0.26 | -1.25 | 2.58 | 1.75 | -1 | 0.15 | -0.56 | 0.20 | -0.42 | Yes |
| 56 | 0 | 14 | -0.26 | 0.13 | -0.41 | 0.36 | 1.95 | -1 | 0.09 | -0.26 | 0.10 | -0.19 | Yes |
| 52 | 90 | 14 | -0.74 | 0.25 | -0.99 | 1.61 | 1.80 | -1 | 0.15 | -0.76 | 0.19 | -0.63 | Yes |
| 54 | 90 | 14 | -0.91 | 0.31 | -1.16 | 1.87 | 1.76 | -1 | 0.19 | -0.94 | 0.24 | -0.77 | No |
| 56 | 90 | 14 | -1.00 | 0.32 | -1.24 | 3.16 | 1.79 | -1 | 0.19 | -1.02 | 0.25 | -0.85 | Yes |
| 52 | 45 | 14 | -1.84 | 0.87 | -0.59 | 0.24 | 1.98 | -1 | 0.61 | -1.86 | 0.68 | -1.45 | No |
| 54 | 45 | 14 | -0.55 | 0.25 | -2.55 | 12.06 | 1.56 | -0.93 | 0.11 | -0.57 | 0.19 | -0.44 | Yes |
| 56 | 45 | 14 | -0.82 | 0.38 | -1.91 | 5.96 | 1.51 | -1 | 0.17 | -0.93 | 0.29 | -0.66 | Yes |

(Note:- [1]: SD - standard deviation, [2]: Skew - skewness, [3]: Kurt – excess kurtosis; [4]: the distribution function of Gumbel minimum is given by $F_X(x) = \exp\left(-\exp\left(\frac{x-\mu}{\gamma}\right)\right); \quad -\infty < x < \infty, \gamma > 0$, [5]: based on stability criterion (see Fig. 6); *: when $\alpha = 2$, the parameter $\beta$ loses its significance)

From Table 1, it is noted that, in almost all the cases considered, the value of skewness parameter ($\beta$) of the alpha-stable distribution is equal to the lower bound value of -1, indicating that the distribution is maximally negatively skewed. This indicates that while the lower tail of the distribution is Paretian (behaves like $|x|^{-\alpha}$ for large $|x|$), the upper tail has no Paretian component. The values of location parameter ($\delta$) of the alpha-stable distribution are found to be in good agreement with the mean (see Fig. 5), which is expected since $\delta$ is the mean of the alpha-stable distribution for cases where $\alpha > 1$ (which is indeed true for the cases considered as can be noted from Table 1).

In order to apply the Hermite polynomial model proposed by Yang *et al*. (2013) and Peng *et al.* (2014), the region of stability in skewness-kurtosis space needs to be established. The stability region along with the pairs of computed skewness and kurtosis values for the wind pressure data considered in this investigation are shown in Fig. 6. From this figure, it is noted that only a subset of the wind pressure data considered are in the stability region. Recent investigations by Peng *et al.* (2014) presented a method to obtain the refined points (for the points slightly away from the stability region) for which Hermite polynomial can be fitted. The possible differences in tail behavior of probability density functions for cases having approximately the same values of skewness and kurtosis but, falling in different regions of Fig. 6, are examined. The histograms of 1 second peak wind pressure coefficients for three sets, with each set having two cases (one inside the effective region of Hermite polynomial model and the other one outside) with comparable values of skewness and kurtosis are shown in Fig. 7. From this figure, it is noted that for the points falling outside the stability region, the rising tails are more pronounced and the tail rises slowly compared to the corresponding points falling within the stability region. Hence, the Hermite polynomial model may not be able to predict the extreme tail information (extreme values of 1-second peak negative wind pressure coefficients in this case). It is noted that the Hermite polynomial approach belongs to a 'model-free' approach and is a non-parametric approach. It disregards the study of underlying process and is completely data-driven, and is highly dependent on the construction architecture of the fitting technique used (Fogarasi 2003). While the recent investigations by Peng *et al.* (2014) can be used to fit the Hermite polynomial for the points falling slightly away from the stability region, this approach would be considered by the authors in the future.

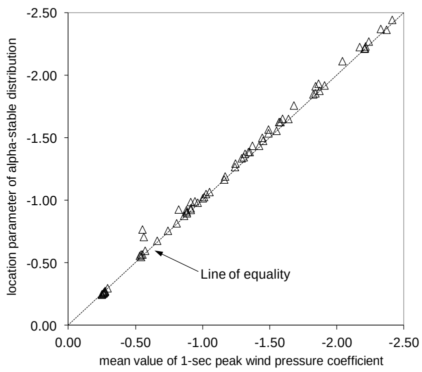


Fig. 5 Comparison of location parameters of alpha-stable distribution with mean values of $\check{C}_p$ (estimated from wind tunnel records)

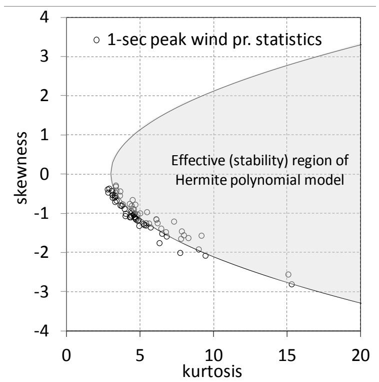


Fig. 6 Skewness and kurtosis for the 1-second peak wind pressure coefficients for the cases considered in the present study (see Table 1) and the effective (stability) region for Hermite polynomial model (Note: *- the value of kurtosis presented in Table 1 is the excess kurtosis, and the kurtosis presented in this figure is obtained by adding 3 to the excess kurtosis)

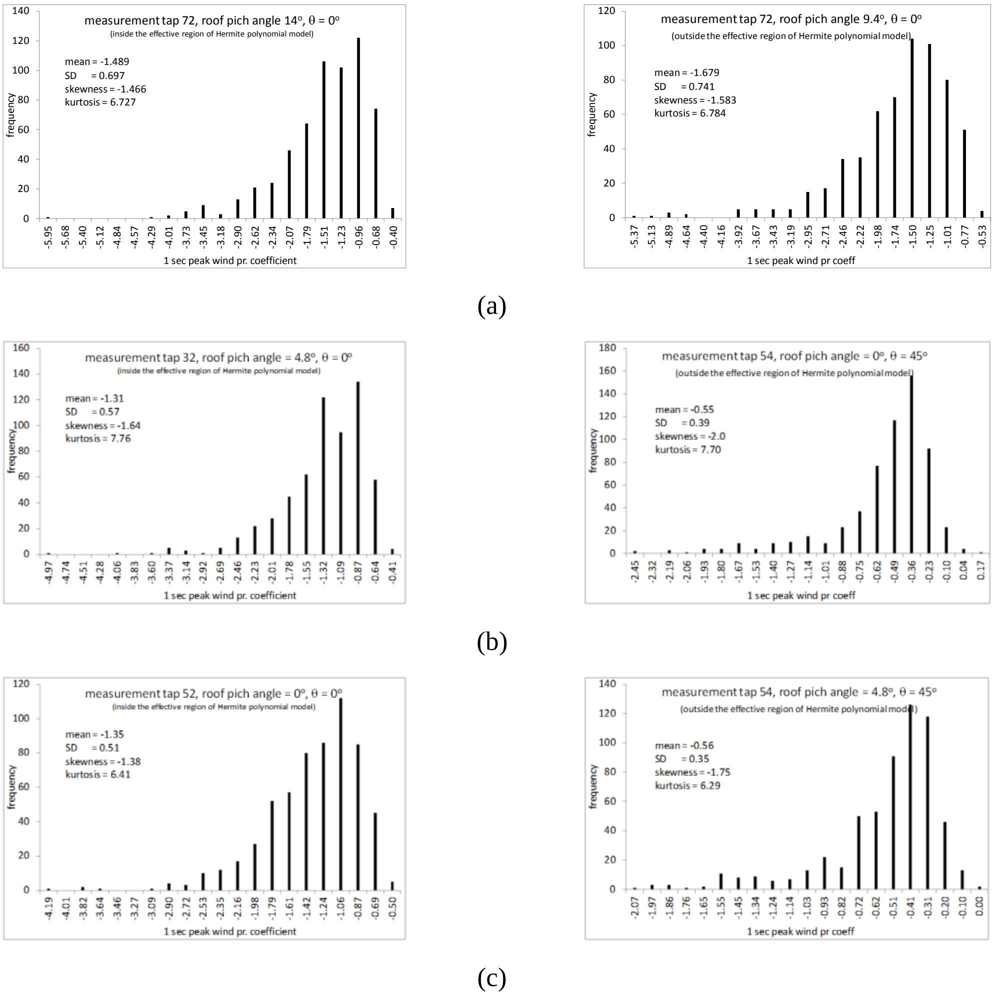


Fig. 7 Comparison of histograms of 1 second peak wind pressure coefficients for three sets, with each set having two cases (one inside the effective region of Hermite polynomial model and the other one outside) with comparable values of skewness and kurtosis

The cumulative distribution functions (cdf) of 1-second peak wind pressure coefficients, for measurement taps 32 and 72, for θ = 0° and θ = 90° and for the roof pitch angles considered, are shown in Figs. 8 and 9, respectively. The cdfs of 1-second peak wind pressure coefficients for measurement taps 72, 52, 32, 73 and 74 for θ = 45° and roof pitch angle = 0° are shown in Fig. 10. The maximum absolute differences between the alpha-stable- and Gumbel- distributions with the probability distribution of observed wind pressure coefficients for the lower tail portion (probability $\leq$ 0.2) are estimated, and are given in Table 2. Since only a subset of the data considered satisfied the stability criterion of Yang *et al*. (2013), the Hermite polynomial-based fit is not considered in this table. However, this approach would be considered by the authors in the future by using the method proposed by Peng *et al*. (2014). From the results given in Table 2 and from the cdfs shown in Figs. 8-10 and similar figures prepared for other measurement taps considered, it is noted that in most of the cases, alpha-stable distribution provides a better estimate of the lower tail portion of peak wind pressure coefficients.

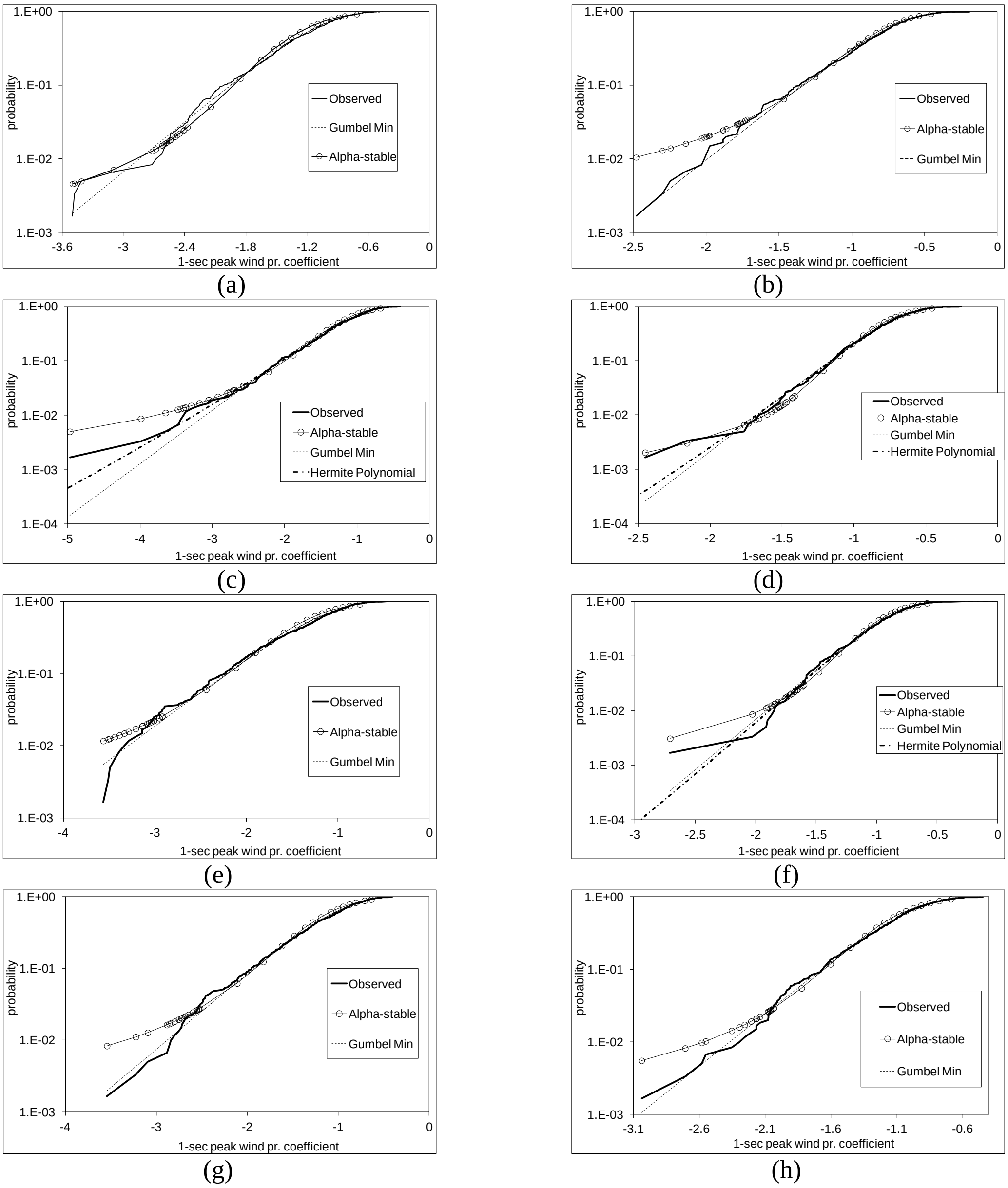


Fig. 8 Comparison of cdfs of 1-second peak wind pressure coefficients for measurement tap 32: (a) roof pitch angle = 0°, θ = 0°; (b) roof pitch angle = 0°, θ = 90°; (c) roof pitch angle = 4.8°, θ = 0°; (d) roof pitch angle = 4.8°, θ = 90°; (e) roof pitch angle = 9.4°, θ = 0°; (f) roof pitch angle = 9.4°, θ = 90°; (g) roof pitch angle = 14°, θ = 0°; (h) roof pitch angle = 14°, θ = 90°

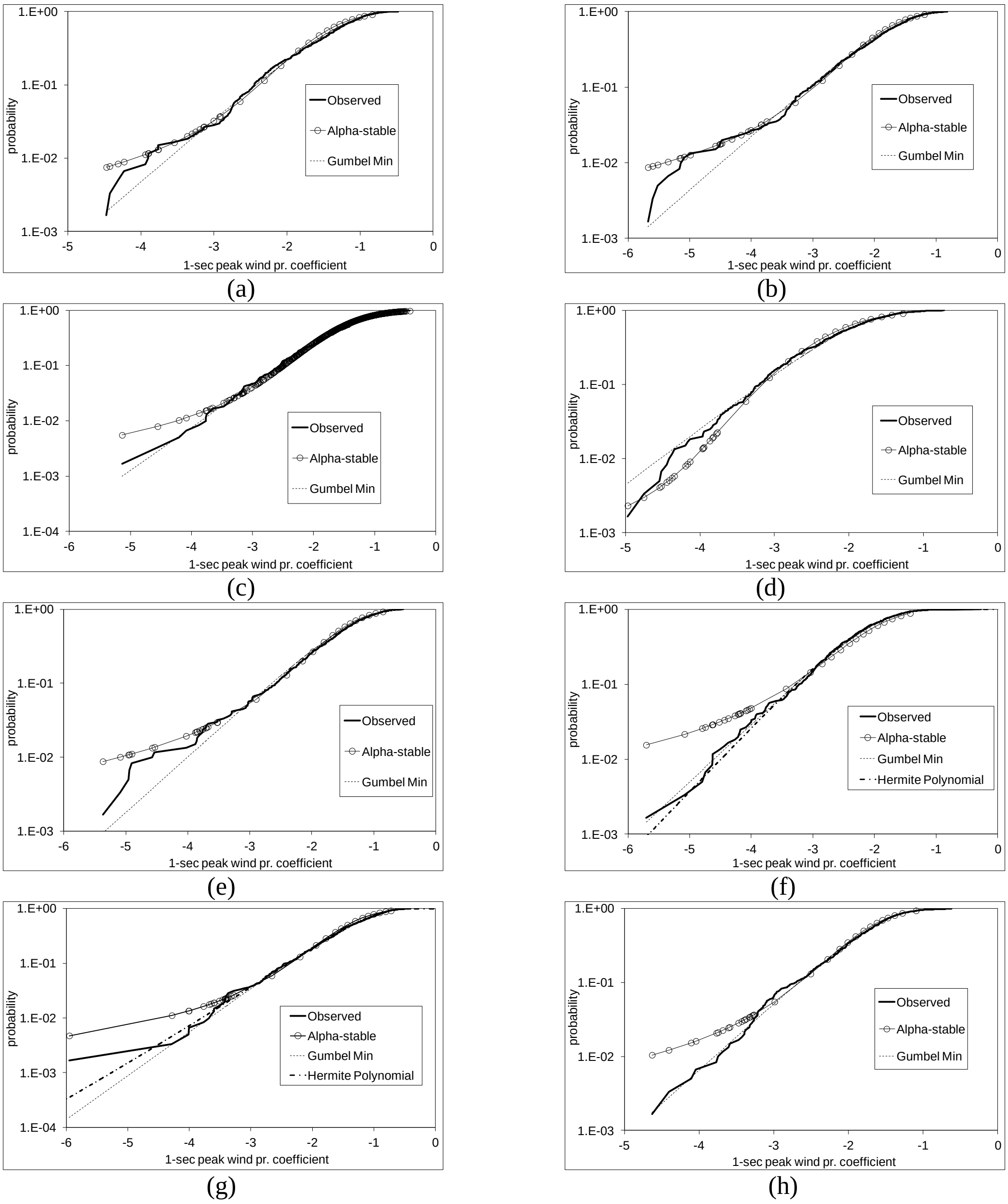


Fig. 9 Comparison of cdfs of 1-second peak wind pressure coefficients for measurement tap 72: (a) roof pitch angle = 0°, θ = 0°; (b) roof pitch angle = 0°, θ = 90°; (c) roof pitch angle = 4.8°, θ = 0°; (d) roof pitch angle = 4.8°, θ = 90°; (e) roof pitch angle = 9.4°, θ = 0°; (f) roof pitch angle = 9.4°, θ = 90°; (g) roof pitch angle = 14°, θ = 0°; (h) roof pitch angle = 14°, θ = 90°

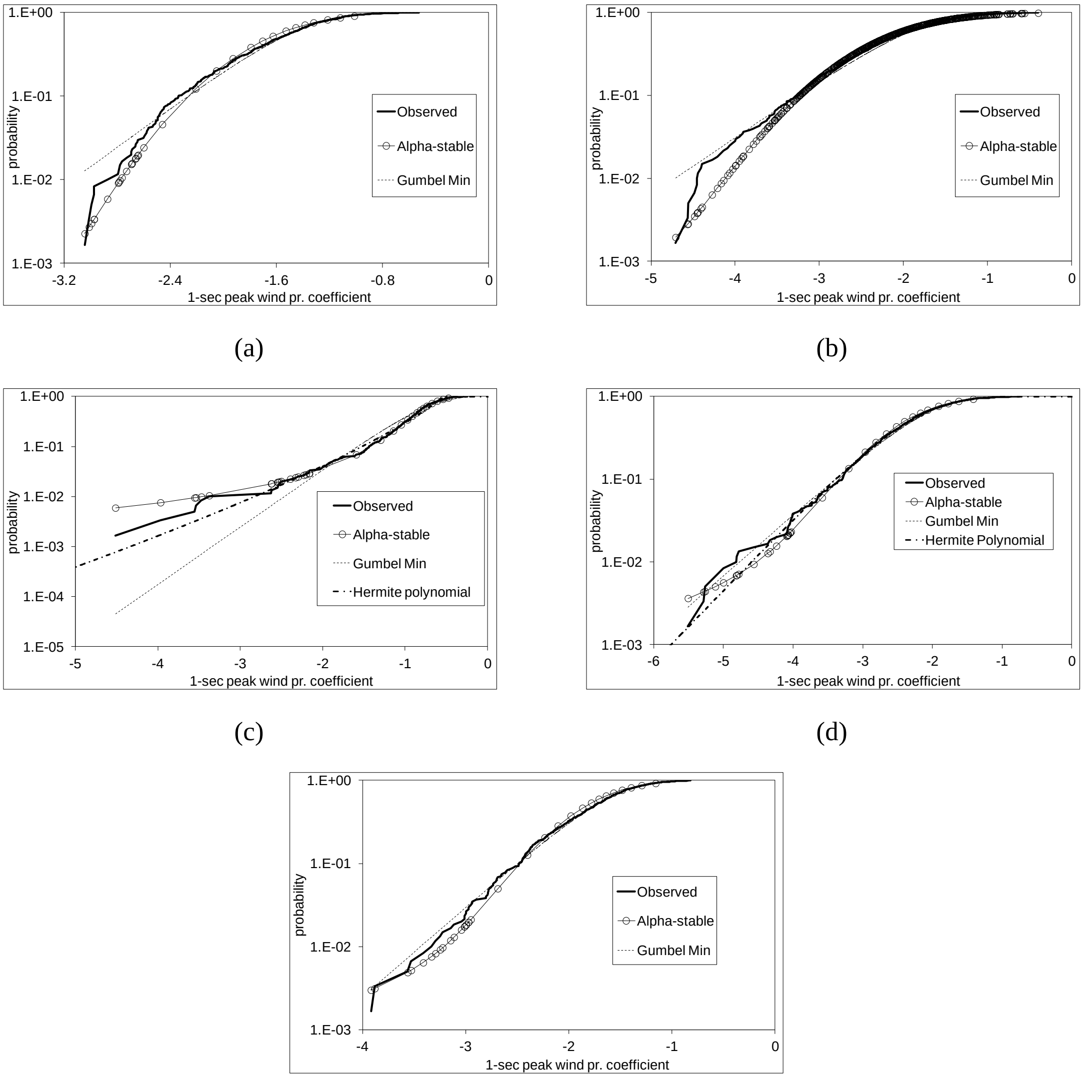


Fig. 10 Comparison of cdfs of 1-second peak wind pressure coefficients for θ = 45° (roof pitch angle = 0°): (a) measurement tap 32; (b) measurement tap 52; (c) measurement tap 72; (d) measurement tap 73; (e) measurement tap 74;

It is known that one of the possibilities for the parent distribution which generates an extreme value distribution is that distribution itself (Ang and Tang 1984). Hence, it is justifiable to make an assumption that the parent distribution of $\check{C}_p$ should have power law decaying tails. This would become evident from the phase plane plot of $C_p$. The plots of $C_p$ versus $\dot{C}_p$ (i.e., the rate of change of $C_p$ with time) corresponding to the measurement taps considered are prepared. The phase plane plots, typically for some of the measurement taps considered, are shown in Figs. 11 and 12. From these figures and similar figures prepared, it is noted that the phase plane plots show large scatter suggesting the need to use probability distributions with heavy tails to model the large pressure fluctuations, which occur due to the jumps observed in the trace of $C_p$ (see Fig. 4(a)). It is also noted that, in general, when the phase plane plot for $C_p$ is symmetrical, the best fitting alpha-stable distribution for $\check{C}_p$ have $\alpha$ values close to 2 (suggesting normal distribution).

Table 2 Fitness of the alpha-stable- and Gumbel- distributions- for the lower tail of probability distribution of observed wind pressure coefficients

| Measurement tap | θ (°) | Roof pitch angle (°) | $max(\lvert F^{fitted}(.) - F^{obs}(.)\rvert)$ for lower tail (i.e., CDF ≤ 0.2) | |
|---|---|---|---|---|
| | | | alpha-stable distribution | Gumbel (min) distribution |
| 32 | 0 | 0 | 0.029 | **0.019** |
| | | 4.8 | **0.021** | 0.023 |
| | | 9.4 | **0.016** | 0.017 |
| | | 14 | **0.013** | 0.014 |
| | 90 | 0 | **0.014** | 0.015 |
| | | 4.8 | 0.016 | **0.015** |
| | | 9.4 | 0.024 | **0.016** |
| | | 14 | 0.017 | **0.012** |
| 51 | 0 | 0 | 0.027 | **0.022** |
| | | 4.8 | **0.012** | 0.014 |
| | | 9.4 | 0.030 | **0.017** |
| | | 14 | **0.015** | 0.022 |
| | 90 | 0 | **0.012** | 0.016 |
| | | 4.8 | 0.023 | **0.014** |
| | | 9.4 | 0.018 | **0.017** |
| | | 14 | **0.019** | 0.023 |
| 72 | 0 | 0 | 0.028 | **0.023** |
| | | 4.8 | **0.024** | 0.026 |
| | | 9.4 | **0.012** | 0.022 |
| | | 14 | **0.015** | 0.017 |
| | 90 | 0 | **0.013** | **0.013** |
| | | 4.8 | **0.014** | 0.024 |
| | | 9.4 | 0.021 | **0.015** |
| | | 14 | **0.019** | 0.020 |
| 82 | 0 | 0 | 0.020 | **0.014** |
| | | 4.8 | **0.012** | 0.019 |
| | | 9.4 | **0.007** | 0.024 |
| | | 14 | 0.014 | 0.025 |
| | 90 | 0 | 0.021 | **0.015** |
| | | 4.8 | **0.019** | 0.038 |
| | | 9.4 | 0.016 | **0.015** |
| | | 14 | 0.019 | 0.032 |

| | | | | |
|---|---|---|---|---|
| 32 | 45 | 0 | **0.025** | 0.035 |
| 52 | 45 | 0 | **0.018** | 0.026 |
| 72 | 45 | 0 | **0.009** | 0.082 |
| 73 | 45 | 0 | **0.014** | 0.018 |
| 74 | 45 | 0 | **0.018** | 0.028 |
| 52 | 0 | 0 | 0.014 | **0.011** |
| 54 | 0 | 0 | 0.019 | **0.014** |
| 56 | 0 | 0 | **0.014** | 0.033 |
| 52 | 90 | 0 | **0.018** | 0.020 |
| 54 | 90 | 0 | 0.022 | **0.016** |
| 56 | 90 | 0 | 0.015 | **0.014** |
| 52 | 45 | 0 | **0.018** | 0.026 |
| 54 | 45 | 0 | **0.035** | 0.081 |
| 56 | 45 | 0 | **0.023** | 0.024 |
| 52 | 0 | 4.8 | **0.013** | 0.021 |
| 54 | 0 | 4.8 | 0.019 | **0.016** |
| 56 | 0 | 4.8 | 0.022 | **0.009** |
| 52 | 90 | 4.8 | 0.027 | **0.021** |
| 54 | 90 | 4.8 | 0.021 | **0.011** |
| 56 | 90 | 4.8 | 0.024 | **0.016** |
| 52 | 45 | 4.8 | 0.024 | **0.008** |
| 54 | 45 | 4.8 | **0.022** | 0.062 |
| 56 | 45 | 4.8 | **0.017** | 0.030 |
| 52 | 0 | 9.4 | **0.015** | 0.020 |
| 54 | 0 | 9.4 | 0.020 | **0.018** |
| 56 | 0 | 9.4 | **0.013** | 0.015 |
| 52 | 90 | 9.4 | 0.023 | **0.020** |
| 54 | 90 | 9.4 | **0.012** | 0.015 |
| 56 | 90 | 9.4 | 0.021 | **0.015** |
| 52 | 45 | 9.4 | **0.022** | 0.030 |
| 54 | 45 | 9.4 | **0.019** | 0.048 |
| 56 | 45 | 9.4 | 0.017 | **0.016** |
| 52 | 0 | 14 | 0.013 | **0.011** |
| 54 | 0 | 14 | 0.023 | **0.015** |
| 56 | 0 | 14 | 0.030 | **0.010** |
| 52 | 90 | 14 | 0.029 | **0.016** |
| 54 | 90 | 14 | **0.013** | 0.014 |
| 56 | 90 | 14 | **0.009** | 0.015 |
| 52 | 45 | 14 | 0.030 | **0.027** |
| 54 | 45 | 14 | **0.021** | 0.075 |
| 56 | 45 | 14 | **0.043** | 0.050 |

(Note: * - since the Hermite polynomial model is not applicable for most of the cases considered in the present study, the same is not considered while identifying the best fitting probability distribution)

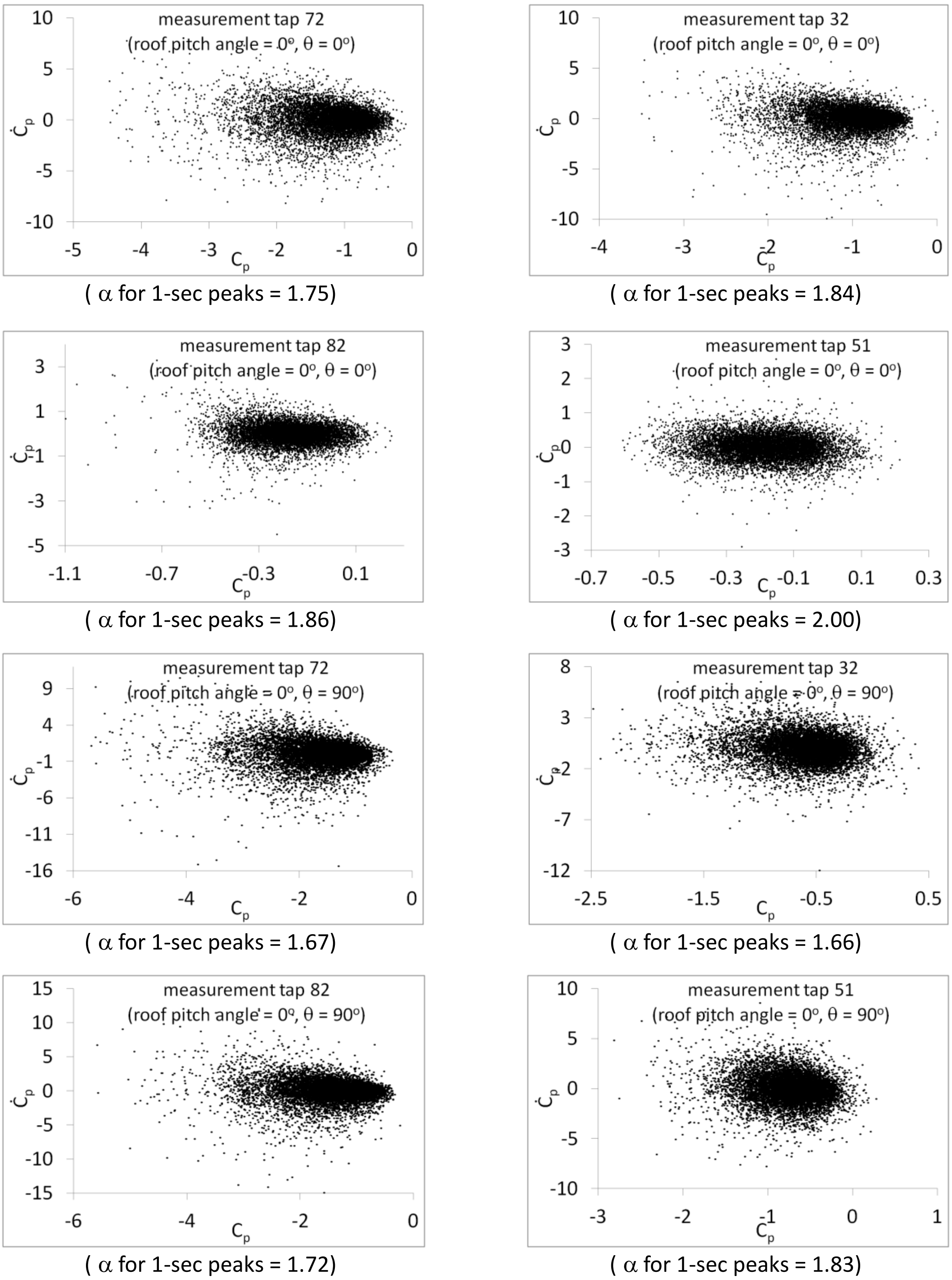


Fig. 11 Phase plane plots of wind pressure coefficients for different measurement taps (roof pitch angle = 0°)

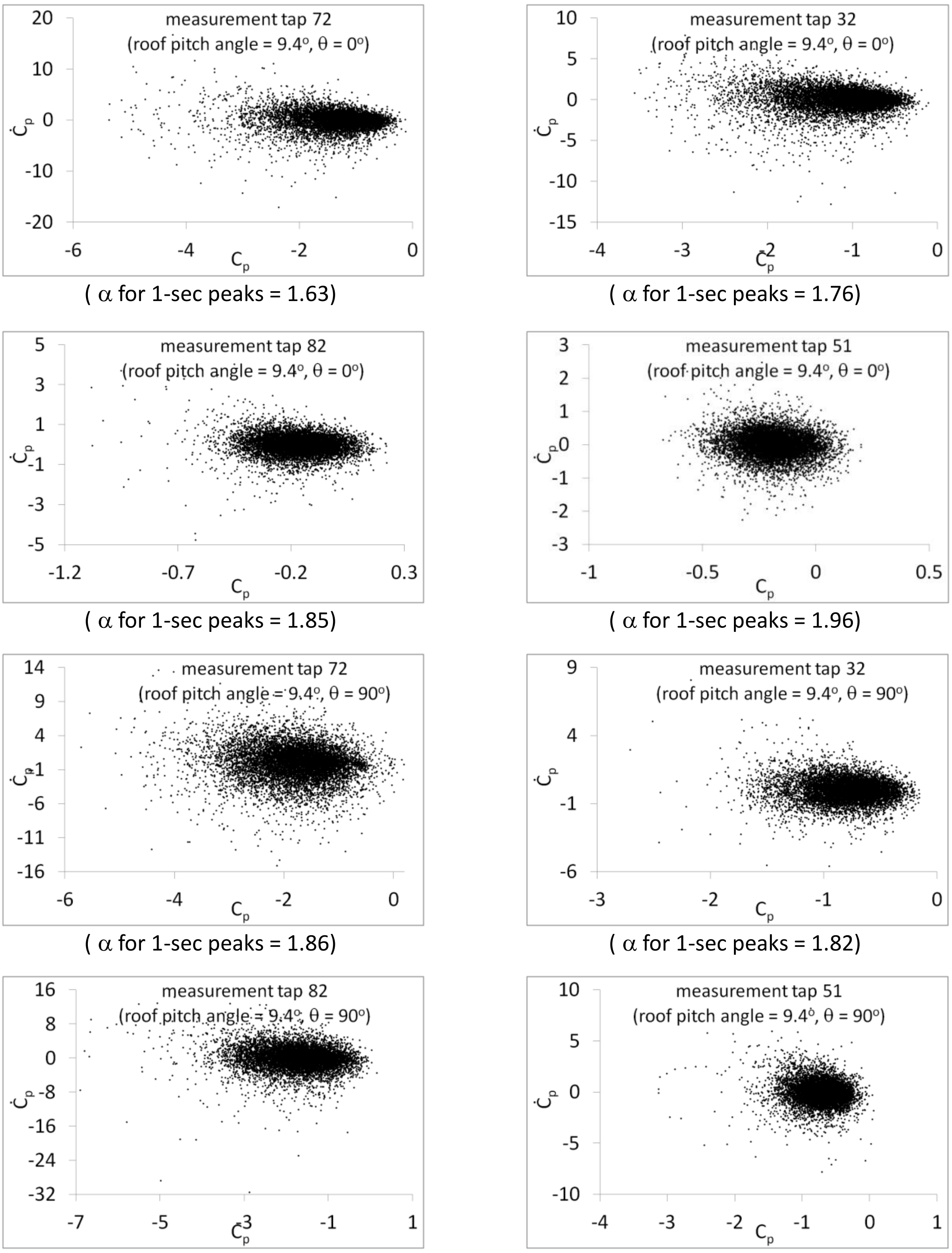


( α for 1-sec peaks = 1.63) ( α for 1-sec peaks = 1.76)

( α for 1-sec peaks = 1.85) ( α for 1-sec peaks = 1.96)

( α for 1-sec peaks = 1.86) ( α for 1-sec peaks = 1.82)

( α for 1-sec peaks = 1.81) ( α for 1-sec peaks = 1.81)

Fig. 12 Phase plane plots of wind pressure coefficients for different measurement taps (roof pitch angle = 9.4°)

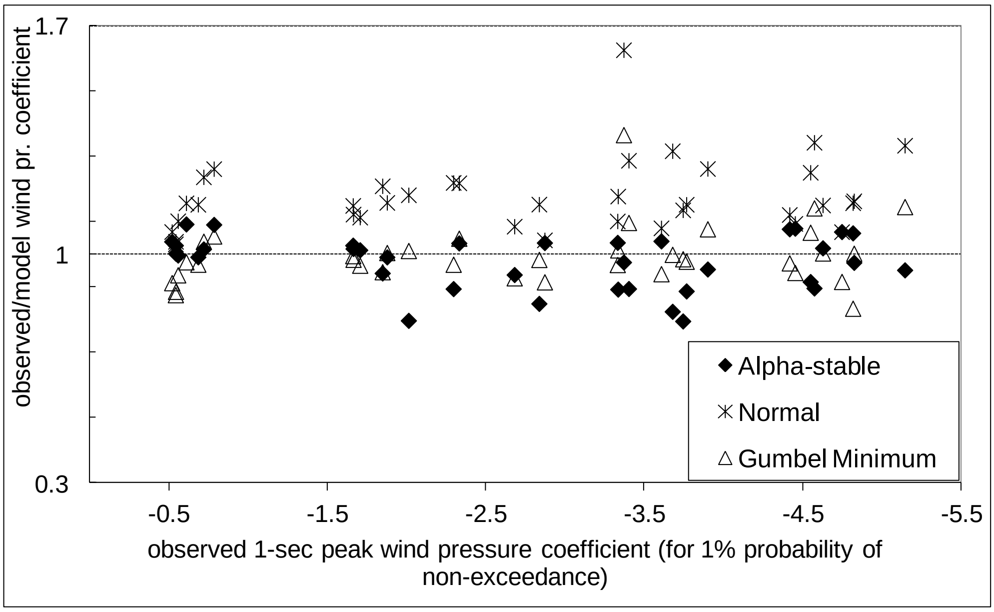


Fig. 13 Ratio of observed- to model- 1-second peak wind pressure coefficients corresponding to 1% probability of non-exceedance

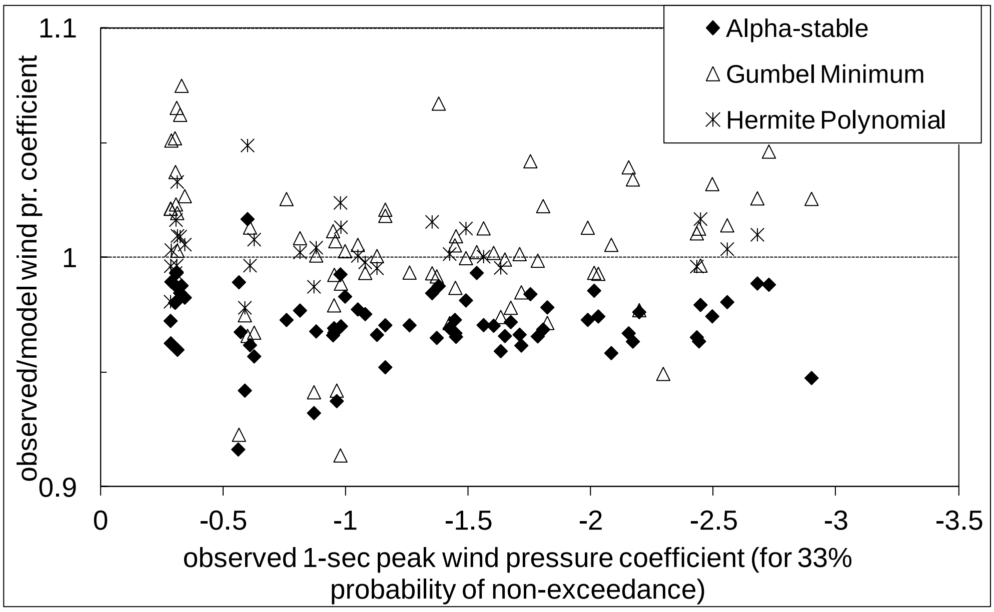


Fig. 14 Ratio of observed- to model-1-second peak wind pressure coefficients corresponding to 33% probability of non-exceedance

To study the efficacy of alpha-stable distribution in modeling the lower tail portion of peak wind pressure coefficients, the values of $\check{C}_p$, typically corresponding to 1%- and 33%- probability of non-exceedance are determined. The ratio between observed- and model- of 1-second peak wind pressure coefficients corresponding to 1%- and 33%- probability of non-exceedance are shown in Figs. 13 and 14. In Figs. 13 and 14, '*model*' denote the values of 1-sec peak wind pressure coefficients corresponding to the probability of non-exceedance considered assuming $\check{C}_p$ follows alpha-stable-, Gumbel minimum- or Hermite polynomial-based model (where applicable)- distribution. From these figures, it is noted that:

i. For 1% probability of non-exceedance (Fig. 13), the Gumbel minimum distribution gives conservative estimates of $\check{C}_p$ when the values of $\check{C}_p$ are low (less than 1.0). For higher values of $\check{C}_p$, the alpha-stable distribution gives conservative estimates of $\check{C}_p$. The performance of the Hermite polynomial-based model is comparable with that of alpha-stable distribution.

ii. For 33% probability of non-exceedance (Fig. 14), the alpha-stable distribution give conservative estimates of $\check{C}_p$ regardless of the value of $\check{C}_p$. The Gumbel minimum distribution gives lower estimates of $\check{C}_p$ for most of the cases. The performance of the Hermite polynomial-based model is comparatively better than the performances of the alpha-stable distribution and the Gumbel minimum distribution.

The above results suggest that to predict maximum suction wind pressure coefficients, alpha-stable distribution is a suitable candidate distribution. The alpha-stable distribution has an advantage that it is consistent with the physical processes proposed in the literature for explaining large fluctuations at the roof corners. The generality and flexibility offered by alpha-stable distribution makes it a candidate distribution as a single model (Fama and Roll 1968) for predicting the extreme values of negative peak wind pressure coefficients at different regions on the building roof. The alpha-stable distribution can be used to estimate the extreme peak negative wind pressure coefficients.

## 8. Conclusions

In this paper, the alpha-stable distribution is proposed for prediction of peak wind pressure coefficients on roofs of low-rise buildings. The use of alpha-stable distribution is justified through its generality (generalized central limit theorem) and the physics of non-Gaussian diffusion process. The fit of alpha-stable distribution for peak wind pressure coefficients is explored using wind tunnel experiment data obtained from the aerodynamic database of Tokyo Polytechnic University. The predictions are compared with those actually measured during wind tunnel experiments, and those predicted by using Gumbel minimum and Hermite polynomial-based model (where applicable). From the comparisons, it is noted that the proposed model can be used to estimate the peak negative wind pressure coefficients.

## Acknowledgements

This paper is being published with the kind permission of the Director, CSIR-SERC, Chennai. The authors are grateful to Prof. R. Narasimha, Chairman, Engineering Mechanics Unit, JNCASR and Director, National Institute of Advanced Studies, Bangalore, and, an internationally renowned expert in fluid dynamics, for providing relevant literature that helped the authors to gain fluid dynamics expert insights into the phenomenon considered in this paper. The MATLAB programs developed and made available in the public domain by Mark Veillette, Ph.D. Scholar, Department of Mathematics and Statistics, Boston University, Boston, USA, have been used in the present study for determining the parameters and cdfs of the alpha-stable distributions. The authors are thankful to the reviewer for giving insightful comments.

## References

Ang, A.H.S. and Tang, W.H. (1984), *Probability Concepts in Engineering Planning and Design, Vol. II*, John Wiley and Sons, New York.

Balaji Rao, K., Anoop, M.B., Kesavan, K., Balasubramanian, S.R., Ravisankar, K. and Nagesh R., Iyer (2013), "Modelling of strains in reinforced concrete flexural members using alpha-stable distribution", *Comput. Concrete*, **11**(5), 411-440.

Banks, D. and Meroney, R.N. (2001), "The applicability of quasi-steady theory to pressure statistics beneath roof-top vortices", *J. Wind Eng. Ind. Aerod.*, **89**(6), 569-598.

Banks, D., Meroney, R.N., Sarkar, P.P., Zhao, Z. and Wu, F. (2000) "Flow visualization of conical vortices on flat roofs with simultaneous surface pressure measurement", *J. Wind Eng. Ind. Aerod.*, **84**(1), 65-85.

Bates, S. and McLaughlin, S. (2000), "The estimation of stable distribution parameters from teletraffic data", *IEEE T. Signal Proces.*, **48**(3), 865-870.

Bienkiewicz, B. and Sun, Y. (1992), "Local wind loading on the roof of a low-rise building", *J. Wind Eng. Ind. Aerod.*, **45**(1), 11-24.

Blazewicz, A.M. (2007), *On the relation between fluid flow over bluff bodies and accompanying acoustic radiation*, Ph. D. Thesis, School of Mechanical Engineering, The University of Adelaide, Australia.

Cope, A.D., Gurley, K.R., Gioffre, M. and Reinhold T.A. (2005), "Low-rise gable roof wind loads: characterization and stochastic simulation", *J. Wind Eng. Ind. Aerod.*, **93**(9), 719-738.

Fama, E.F. and Roll, R. (1968), "Some properties of symmetric stable distributions", *J. Am. Statist. Assoc.*, **63**(323), 817-836.

Fogarasi, N. (2003), *Non-Gaussian option pricing*, Technical report, http:// www.hit.bme.hu/~fogarasi (last accessed on 4 April 2014).

Ginger, J.D. and Fricke, H.W. (2012), "APEC-WW structural report: Australia – 2011-12", *Proceedings of the Workshop on regional harmonization of wind loading and wind environmental specifications in Asia-Pacific economies (APEC-WW2012)*, Hanoi.

Holmes, J.D. and Cochran, L.S. (2003), "Probability distributions of extreme pressure coefficients", *J. Wind Eng. Ind. Aerod.*, **91**(7), 893-901.

Kareem, A. (2010), "Bluff body aerodynamics and aeroelasticity: a wind effects perspective", *J. Wind Eng. Ind. Aerod.*, **7**(1), 30-74.

Kawai, H. and Nishimura, G. (1996), "Characteristics of fluctuating suction and conical vortices on a flat roof in oblique flow", *J. Wind Eng. Ind. Aerod.*, **60**, 211-225.

Kogon, S.M. and Williams D.B. (1995), "On the characterization of impulsive noise with alpha-stable distributions using Fourier techniques", *Proceedings of the 29$^{th}$ Asilomar Asilomar Conference on Signals*, Systems and Computers.

Koutrouvelis, I.A. (1980), "Regression-type estimation of the parameters of stable laws", *J. Am. Statist. Assoc.*, **75**(372), 918-928.

Kumar, K.S. and Stathopoulos T. (2000) "Wind loads on low building roofs: a stochastic perspective", *J. Struct.Eng. - ASCE*, **126**(8), 944-956.

Li, Q.S., Calderone, I. and Melbourne, W.H. (1999), "Probabilistic characteristics of pressure fluctuations in separated and reattaching flows for various free-stream turbulence", *J. Wind Eng. Ind. Aerod.*, **82**(1-3), 125-145.

Lindenberg, K. and West, B.J. (1990), *The nonequilibrium statistical mechanics of open and closed systems*, VCH Publishing Inc., New York.

Ma, X. and Nikias, C.L. (1995), “Parameter estimation and blind channel identification in impulsive signal environments”, *IEEE T. Signal Proces.*, **43**(12), 2884-2897.

McCulloch, J.H. (1986), “Simple consistent estimators of stable distribution parameters”, *Commun. Stat. – Simul. C.*, **15**(4), 1109-1136.

Melbourne, W.H. (1980), “Turbulence, bluff body aerodynamics and wind engineering”, *Proceedings of the7th Australasian hydraulics and fluid mechanics conference*, Brisbane.

Melbourne, W.H. (1993), “Turbulence and the leading edge phenomenon”, *J. Wind Eng. Ind. Aerod.*, **49**(1-3), 45-64.

Metzler, R. and Klafter, J. (2004), “The restaurant at the end of the random walk: recent”developments in the description of anomalous transport by fractional dynamics”, *J. Phys. A- Math. Gen.*, **37**(31), 161-208.

Narasimha, R., Rudra Kumar, S., Prabhu, A. and Kailas, S.V. (2007), “Turbulent flux events in a nearly neutral atmospheric boundary layer”, *Philos. T. R. Soc. A*, **365**(1852), 841-858.

Nolan, J.P. (2009), *Stable Distributions: Models for Heavy Tailed Data*, Boston: BirkhÄ auser. Unfinished manuscript, Chapter 1 online at http://academic2.american.edu/~jpnolan/stable/chap1.pdf (last accessed: 27 August 2013).

Peng, X., Yang, L., Gavanski, E., Gurley, K. and Prevatt, D. (2014), “A comparison of methods to estimate peak wind loads on buildings”, *J. Wind Eng. Ind. Aerod.*, **126**, 11-23.

Tieleman, H.W. (2003), “Wind tunnel simulation of wind loading on low-rise structures: a review”, *J. Wind Eng. Ind. Aerod.*, **91**, 1627-1649.

Tieleman, H.W., Elsayed, M.A.K., Ge, Z. and Hajj, M.R. (2008), “Extreme value distributions for peak pressure and load coefficients”, *J. Wind Eng. Ind. Aerod.*, **96**(6-7), 1111-1123.

TPU (2013), “Aerodynamic database of low-rise buildings”, Tokyo Polytechnic University, *http://www.wind.arch.t-kougei.ac.jp/system/eng/* (last accessed: 27 August 2013).

Tsihrintzis, G.A. and Nikias, C.L. (1996), “Fast estimation of the parameters of alpha-stable impulsive interference”, *IEEE T. Signal Proces.*, **44**(6), 1492-1503.

Wang, B., Kuo, J., Bae, S.C. and Granick, S. (2012), “When Brownian diffusion is not Gaussian”, *Nature Materials*, **11**, 481-485.

Yang, L., Gurley, K. and Prevatt, D.O. (2013), “Probabilistic modeling of wind pressure on low-rise buildings”, *J. Wind Eng. Ind. Aerod.*, **114**, 18-26.

*CC*

## Appendix

### *Estimation of Parameters of Alpha-Stable Distribution*

Different methods have been proposed in literature for the estimations of the parameters $\alpha$, $\beta$, c and $\delta$ of the alpha-stable distribution. Fama and Roll (1968) suggested a quantile-based method for estimation of characteristic exponent and scale parameter of symmetric alpha-stable distributions with $\delta = 0$. However, this method is applicable only for distributions with $\alpha>1$. This method has been modified by McCulloch (1986) to include even non-symmetric distributions with $\alpha$ in the range [0.6, 2.0]. Koutrouvelis (1980) proposed a characteristic function-based method involving an iterative regression procedure for estimation of the parameters of the alpha-stable distribution. Kogon and Williams (1995) improved this method by eliminating the iterative procedure and simplifying the regression. Ma and Nikias (1995) and Tsihrintzis and Nikias (1996) proposed the use of fractional lower order moments (FLOMs) for estimating the parameters of symmetric alpha-stable distributions. Bates and McLaughlin (2000) studied the performances of the methods proposed by McCulloch (1986), Kogon and Williams (1995), Ma and Nikias (1995) and Tsihrintzis and Nikias (1996) using two real data sets. They found that there are marked differences between the results obtained using the different methods. In the present study, the parameters $\alpha$, $\beta$, c and $\delta$ of the alpha-stable distribution are estimated using an optimization procedure by minimizing the sum of squares of the difference between the observed cumulative distribution function (empirical distribution function) and the cumulative distribution function (CDF) of the alpha-stable distribution.

In the present study, the parameters $\alpha$, $\beta$, c and $\delta$ of the alpha-stable distribution are estimated using an optimization procedure by minimizing the sum of squares of the difference between the observed cumulative distribution function (empirical distribution function) and the cumulative distribution function (CDF) of the alpha-stable distribution. The procedure used is as follows:

1. Given the $N$ ordered observed data points $x_1$, $x_2$, $x_3$, …,$x_N$, define the empirical distribution function as

$$E_N(i) = \frac{n(i)}{N+1} \qquad \text{(A-1)}$$

where n(i) is the number of data points less than or equal to $x_i$, and $x_i$ are ordered from smallest to largest value.

2. Define the objective function as

$$Z = \sum_{i=1}^{N} \left( E_N(i) - \tilde{F}_{\alpha S}(x_i;\alpha,\beta,\gamma,\delta) \right)^2 \qquad \text{(A-2)}$$

where $\tilde{F}_{\alpha S}(x_i;\alpha,\beta,\gamma,\delta)$ is the CDF of the alpha-stable distribution. ~ denotes the fact that the form of distribution function is generally not available and has to be approximated numerically.

Determine α, β, c and δ by minimizing *Z* subject to the constraints $0 < \alpha \le 2$, $-1 \le \beta \le 1$ and $c > 0$. In the present study, the minimization is carried out using the constrained nonlinear optimization function available in the software MATLAB. The CDF of the alpha-stable distribution, $\tilde{F}_{\alpha S}\left(x_i;\alpha,\beta,\gamma,\delta\right)$, is computed by numerical integration [23].